

Deeply virtual Compton scattering at small x

IAN BALITSKY and ELENA KUCHINA

Physics Department, Old Dominion University, Norfolk VA 23529

and

Theory Group, Jefferson Lab, Newport News VA 23606

e-mail: balitsky@jlab.org

e-mail: kuchina@jlab.org

Abstract

We calculate the cross section of the deeply virtual Compton scattering at large energies and intermediate momentum transfers.

PACS numbers: 12.38.Bx, 13.85.Fb, 13.85.Ni.

I. INTRODUCTION

In recent years the study of the deeply virtual Compton scattering (DVCS) became one of the most popular topics in QCD due to the fact that it is determined by skewed parton distributions [1-3] which generalize usual parton densities introduced by Feynman. These new probes of the nucleon structure are accessible in exclusive processes such as DVCS and potentially they can give us more information than the traditional parton densities. In this paper we consider the small- x DVCS where the energy of the incoming virtual photon E is very large in comparison to its virtuality Q^2 . (The first study of the small- x DVCS was undertaken in Ref. [4]). To be specific, we calculate the DVCS amplitude in the region

$$s \gg Q^2 \gg -t \gg m^2 \quad (1)$$

where $s = 2mE$, m is the nucleon mass, and t is the momentum transfer. The DVCS in this region is a semihard processes which can be described by the BFKL (Balitsky-Fadin-Kuraev-Lipatov) pomeron [5]. It turns out that at large momentum transfer the coupling of the BFKL pomeron to the nucleon is essentially equal to the Dirac form factor of the nucleon $F_1(t)$, so the DVCS amplitude in the region (1) can be calculated without any model assumptions. The results obtained in this region can be used for the estimates of the amplitude at experimentally accessible energies where one or more conditions in Eq. (1) are relaxed. To be specific, we have in mind the HERA kinematics where $x \sim 10^{-2} \div 10^{-4}$, $Q^2 \geq 6 \text{ GeV}^2$, and $-t \sim 1 \div 5 \text{ GeV}^2$ [6]. Since there are only model predictions for the small- x DVCS in current literature [7], even the approximate calculations of the cross section in QCD are very timely.

II. SMALL- x DVCS IN THE LOWEST ORDER IN PERTURBATION THEORY

Similarly to the case of deep inelastic scattering (DIS), the amplitude of DVCS is determined by the matrix element [8]

$$H^{AB} = ie_\nu^A e_\mu^B \int dz e^{iq'z} \langle p' | T \{ j^\mu(z) j^\nu(0) \} | p \rangle \quad (2)$$

where q, p and q', p' are the initial and the final momenta of the photon and the nucleon, respectively. The momentum transfer is defined as $r = p' - p$. Since $Q^2 = -q^2$ is large we can use perturbation theory for the hard part of the DVCS process [9] [10]. The typical diagram for the DVCS amplitude in the lowest order in perturbation theory is shown in Fig.1 (recall that the diagrams with gluon exchanges dominate at high energies). It is convenient

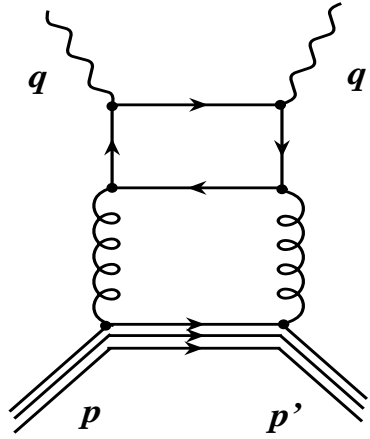


FIG. 1. A typical Feynman diagram for the high-energy $\gamma^* p \rightarrow \gamma p$ scattering

to calculate at first the imaginary part of the amplitude H^{AB}

$$V^{AB} = \frac{1}{\pi} \text{Im} T^{AB}. \quad (3)$$

In the leading order in perturbation theory the amplitude at high energy is purely imaginary up to the $\frac{Q^2}{s}$ corrections (see e.g. the review [11]). At high orders in perturbation theory the amplitude will be purely imaginary in the leading logarithmic approximation (LLA) and we will restore the real part using the dispersion relations.

At high energies it is convenient to use the Sudakov variables. Let us define the light-like vectors $p_1 = q'$, $p_2 = p' - \frac{m^2}{s} p_1$, then

$$q = p_1 \left(1 - \frac{r_\perp^2}{s}\right) - x p_2 - r_\perp \quad q' = p_1$$

$$p = p_2(1+x) + \frac{m^2 + r_\perp^2}{s}p_1 + r_\perp \quad p' = p_2 + \frac{m^2}{s}p_1 \quad (4)$$

where $x \equiv \frac{Q^2+t}{s} \simeq \frac{Q^2}{s} = x_{Bj}$ and $t \simeq -r_\perp^2$ at large energies. Consider the integral over gluon momentum $k = \alpha_k p_1 + \beta_k p_2 + k_\perp$

$$V^{AB} = \frac{2}{\pi} g^4 \int \frac{d^4 k}{16\pi^4} \frac{1}{k^2} \frac{1}{(r+k)^2} \text{Im} \Phi_{\xi\eta}^{ab}(k+r, -k) \text{Im} \Phi_N^{\xi\eta ab}(-k-r, k) \quad (5)$$

where $\Phi_{\xi\eta}^{ab}(k, r+k)$ and $(\Phi_N)^{ab}_{\xi\eta}(k, r+k)$ are the upper and the lower blocks of the diagram in Fig. 2 (stripped of the strong coupling constant g). Here a, b and ξ, η are the color and Lorentz indices, respectively. It is well known that in the Regge kinematics ($\equiv s \gg$

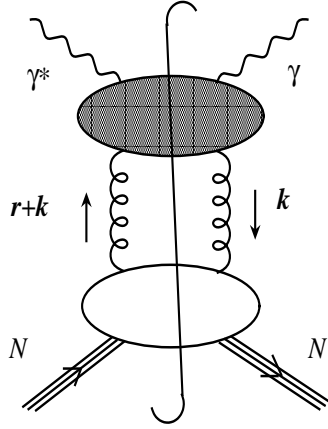


FIG. 2. Block structure of small-x DVCS in the leading order in perturbation theory

everything else) $\alpha_k \sim \frac{m^2}{s}$, and $\beta_k \sim x$ so $k^2 \simeq -k_\perp^2$. Moreover, α 's in the upper block are ~ 1 so one can drop α_k in the upper block. Similarly, β 's in the lower block are ~ 1 and one can neglect β_k in the lower block. We get ($\Phi^{ab} = \frac{\delta_{ab}}{8} \Phi^{cc}$):

$$V^{AB} = \frac{g^4}{4\pi} \int \frac{d^4 k}{16\pi^4} \frac{1}{k_\perp^2} \frac{1}{(r+k)_\perp^2} \text{Im} \Phi_{\xi\eta}^{aa}(k+r, -k) \Big|_{\alpha_k=0} \text{Im} \Phi_N^{\xi\eta bb}(-k-r, k) \Big|_{\beta_k=0}. \quad (6)$$

At high energies, the metric tensor in the numerator of the Feynman-gauge gluon propagator reduces to $g^{\mu\nu} \rightarrow \frac{2}{s} p_2^\mu p_1^\nu$ so the integral (6) for the imaginary part factorizes into a product of two “impact factors” integrated with two-dimensional propagators

$$V^{AB} = \frac{2s}{\pi} g^4 \left(\sum e_q^2 \right) \int \frac{d^2 k_\perp}{4\pi^2} \frac{1}{k_\perp^2} \frac{1}{(r+k)_\perp^2} I(k_\perp, r_\perp) I_N(k_\perp, r_\perp) \quad (7)$$

where

$$I(k_\perp, r_\perp) = \frac{1}{2s} p_2^\xi p_2^\eta \left(\sum e_q^2 \right) \int \frac{d\beta_k}{2\pi} \text{Im} \Phi_{\xi\eta}^{aa}(k+r, -k) \Big|_{\alpha_k=0} \quad (8)$$

$$I_N(k_\perp, r_\perp) = \frac{1}{2s} p_1^\xi p_1^\eta \int \frac{d\alpha_k}{2\pi} \text{Im} \Phi_{N\xi\eta}^{aa}(-k-r, k) \Big|_{\beta_k=0} \quad (9)$$

and $(\sum e_q^2)$ is the sum of squared charges of active flavors (u, d, s , and possibly c). The photon impact factor is given by the two one-loop diagrams shown in Fig. 3. The standard

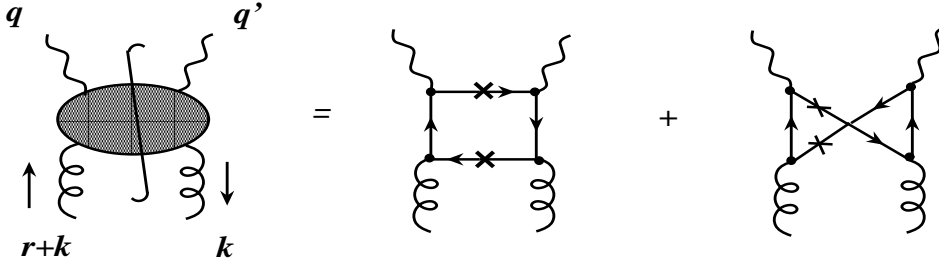


FIG. 3. Photon impact factor

calculation of these diagrams [12] yields

$$I^{AB}(k_\perp, r_\perp) = \bar{I}^{AB}(k_\perp, r_\perp) - \bar{I}^{AB}(0, r_\perp) \quad (10)$$

where

$$\bar{I}^{AB}(k_\perp, r_\perp) = \frac{1}{2} \int_0^1 \frac{d\alpha}{2\pi} \int_0^1 \frac{d\alpha'}{2\pi} \left\{ P_\perp^2 \alpha' \bar{\alpha}' + Q^2 \alpha' \alpha \bar{\alpha} \right\}^{-1} \quad (11)$$

$$\left\{ (1 - 2\alpha\bar{\alpha}) P_\perp^2 (e^A, e^B)_\perp + 4\alpha\bar{\alpha}\bar{\alpha}' [P_\perp^2 (e^A, e^B) - 2(e^A, P)_\perp (e^B, P)_\perp] - 4\alpha\bar{\alpha}(1 - 2\alpha)(r, e^A)_\perp (P, e^B)_\perp \right\}$$

for the transverse polarizations $A, B = 1, 2$ (cf. [13]) and

$$\bar{I}^{3B}(k_\perp, r_\perp) = \frac{1}{2Q} \int_0^1 \frac{d\alpha}{2\pi} \int_0^1 \frac{d\alpha'}{2\pi} \left\{ P_\perp^2 \alpha' \bar{\alpha}' + Q^2 \alpha' \alpha \bar{\alpha} \right\}^{-1} \quad (12)$$

$$\left\{ (1 - 2\alpha\bar{\alpha}) P_\perp^2 (r, e^B)_\perp + 4\alpha\bar{\alpha}\bar{\alpha}' [P_\perp^2 (r, e^B)_\perp - 2(r, P)_\perp (e^B, P)_\perp] - 4\alpha\bar{\alpha}(1 - 2\alpha) Q^2 (P, e^B)_\perp \right\}$$

for the longitudinal polarization

$$e^3(q) = \frac{1}{Q} (p_1 + x p_2) \quad (13)$$

. Here $P_\perp \equiv k_\perp + r_\perp \alpha$ and $(a, b)_\perp$ denotes the (positive) scalar product of transverse components of vectors a and b . At large transverse momenta $k_\perp^2 \gg r_\perp^2$ the impact factor (10) reduces to

$$I^{AB}(k_\perp, r_\perp) \rightarrow \frac{(e^A, e^B)_\perp}{4\pi^2} \frac{k_\perp^2}{Q^2} \ln \frac{Q^2}{r_\perp^2}. \quad (14)$$

The impact factor for the proton which describes the pomeron-nucleon coupling cannot be calculated in the perturbation theory. However, in the next section we demonstrate that at high momenta $k_\perp^2 \gg m^2$ this impact factor reduces to

$$I_N(k_\perp, r_\perp) \stackrel{k_\perp^2 \gg m^2}{=} F_1^{p+n}(t) \quad (15)$$

where $F_1^{p+n}(t)$ is the sum of the proton and neutron Dirac form factors. As we shall see below, the characteristic transverse momenta in our gluon loop are large so the estimate (15) is sufficient for our purposes. Substituting the nucleon impact factor (15) into Eq. (7) we obtain

$$V^{AB} = \frac{2s}{\pi} g^4 (\sum e_q^2) F_1^{p+n}(t) \int \frac{d^2 k_\perp}{4\pi^2} \frac{I^{AB}(k_\perp, r_\perp)}{k_\perp^2 (r + k)_\perp^2}. \quad (16)$$

Performing the final integration over k_\perp , one gets

$$\begin{aligned} V^{AB} = & \frac{2}{x} \left(\frac{\alpha_s}{\pi} \right)^2 \left(\sum_{\text{flavors}} e_q^2 \right) F_1^{p+n}(t) \\ & \left((e^A, e^B)_\perp \left(\frac{1}{2} \ln^2 \frac{Q^2}{|t|} + 2 \right) - (e^A, e^B)_\perp + \frac{2}{r_\perp^2} (e^A, r)_\perp (e^B, r)_\perp + O(t/Q^2) \right) \end{aligned} \quad (17)$$

for the transverse polarizations and

$$\begin{aligned} V^{3B} = & -\frac{2}{x} \left(\frac{\alpha_s}{\pi} \right)^2 \left(\sum_{\text{flavors}} e_q^2 \right) F_1^{p+n}(t) \frac{(r, e^B)_\perp}{Q} \left(\frac{1}{2} \ln^2 \frac{Q^2}{|t|} - 5 \ln \frac{Q^2}{|t|} + \frac{15}{2} - \frac{\pi^2}{3} + O(t/Q^2) \right) \end{aligned} \quad (18)$$

for the longitudinal one. The longitudinal amplitude (18) is twist-suppressed as $\frac{\sqrt{|t|}}{Q}$ in comparison to the transverse amplitude (17) (as it should, due to the fact that $t \rightarrow 0$ corresponds to real incoming photon).

Since the integral over k_\perp (16) converges at $k_\perp \sim Q$ the region $k_\perp \sim m$, where we do not know the nucleon impact factor, contributes to the terms $\sim O(t/Q^2)$ which we neglect.

III. NUCLEON IMPACT FACTOR

In the lowest order in perturbation theory there is no difference between the diagrams for the nucleon impact factor shown in Fig. 4 and similar diagrams with two gluons replaced

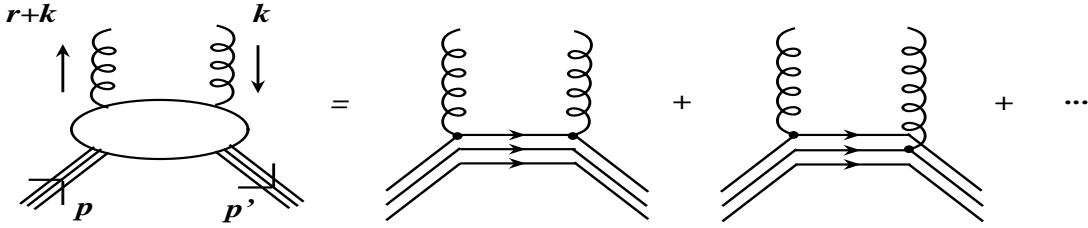


FIG. 4. Nucleon impact factor

by two photons (up to the trivial numerical factor $c_F = \frac{4}{3}$ and replacement of $e \leftrightarrow g$). In this case the lower part of the diagram can be formally written as follows:

$$\Phi_N(-k-r, k) \stackrel{\text{def}}{=} \frac{1}{2} \frac{p_1^\xi p_1^\eta}{s} (\Phi_N)_{\xi\eta}^{bb}(-k-r, k) = \frac{2}{3} i p_1^\mu p_1^\nu \int dz e^{ikz} \langle p' | T^* \{ J_\mu(z) J_\nu(0) \} | p \rangle \quad (19)$$

where $J_\mu = \bar{u} \gamma_\mu u + \bar{d} \gamma_\mu d$. The T^* means the T-product where the diagrams with pure gluon exchanges in t-channel are excluded; by definition, such diagrams contribute to subsequent ranks of BFKL ladder rather than to impact factor. (This is the reason why we have not included in J the contribution of strange quarks). Since k^2 in our case is large and negative ($-k^2 = k_\perp^2 \gg m^2$) we can expand the T-product of two currents near the light cone (see e.g. [14])

$$\Phi_N(k, r+k) = \frac{2}{3s} \int dz e^{ikz} \frac{z p_1}{\pi^2 z^4} \langle p' | -\bar{\psi}(z)[z, 0] \not{p}_1 \psi(0) + \bar{\psi}(0)[0, z] \not{p}_1 \psi(z) | p \rangle_{z^2=0}^* \quad (20)$$

where again $\langle \dots \rangle^*$ stands for the matrix element with pure gluon exchanges excluded. Here $[x, y]$ denotes the gauge link connecting the points x and y ($[x, y] \equiv$

$Perp\left(ig\int_0^1 du(x-y)^\mu A_\mu(ux+(1-u)y)\right)$. The matrix element (16) can be parametrized in terms of skewed parton distributions [9] as follows

$$\begin{aligned} \langle p', \lambda' | \bar{q}(z)[z, 0] \not{p}_1 q(0) | p, \lambda \rangle_{z^2=0}^* = \\ \bar{u}(p', \lambda') \not{p}_1 u(p, \lambda) \int_0^1 dX e^{i(X-x)pz} \mathcal{V}_x^q(X, t) + \frac{1}{2m} \bar{u}(p', \lambda') \not{p}_1 \not{\epsilon}_\perp u(p, \lambda) \int_0^1 dX e^{i(X-x)pz} \mathcal{W}_x^q(X, t) \\ \langle p', \lambda' | \bar{q}(0)[0, z] \not{p}_1 q(z) | p, \lambda \rangle_{z^2=0}^* = \\ \bar{u}(p', \lambda') \not{p}_1 u(p, \lambda) \int_0^1 dX e^{-iXpz} \mathcal{V}_x^q(X, t) + \frac{1}{2m} \bar{u}(p', \lambda') \not{p}_1 \not{\epsilon}_\perp u(p, \lambda) \int_0^1 dX e^{-iXpz} \mathcal{W}_x^q(X, t), \end{aligned} \quad (21)$$

where $\mathcal{V}_x^u(X, t)$ and $\mathcal{W}_x^u(X, t)$ are the nonflip and spin-flip skewed parton distributions for the *valence* u quark (recall that we must take into account only valence quarks since we forbid diagrams with pure gluon exchanges). Similarly, $\mathcal{V}_x^d(X, t)$ and $\mathcal{W}_x^d(X, t)$ refer to the valence d -quark distributions. At large energies $\bar{u}(p', \lambda') \not{p}_1 u(p, \lambda) = s\delta_{\lambda\lambda'}$, so

$$\begin{aligned} \langle p', \lambda' | \bar{q}(0)[0, z] \not{p}_1 q(z) - \bar{q}(z)[z, 0] \not{p}_1 q(0) | p, \lambda \rangle_{z^2=0}^* = \\ \int_0^1 dX \left(e^{-iXpz} - e^{i(X-x)pz} \right) \left[s\delta_{\lambda\lambda'} \mathcal{V}_x^q(X, t) + \frac{1}{2m} \bar{u}(p', \lambda') \not{p}_1 \not{\epsilon}_\perp u(p, \lambda) \mathcal{W}_x^q(X, t) \right]. \end{aligned} \quad (22)$$

After integration over z the lower block (19) reduces to

$$\begin{aligned} \Phi_N(-k-r, k) = \\ \frac{2}{3s} \int_0^1 dX \left[\frac{(X-x)s + 2p_1 \cdot k}{-k^2 - 2p \cdot k(X-x) - i\epsilon} - \frac{-Xs + 2p_1 \cdot k}{-k^2 + 2p \cdot kX - i\epsilon} \right] \\ \left(\delta_{\lambda\lambda'} (\mathcal{V}_x^u(X, t) + \mathcal{V}_x^d(X, t)) + \frac{1}{2ms} \bar{u}(p', \lambda') \not{p}_1 \not{\epsilon}_\perp u(p, \lambda) (\mathcal{W}_x^u(X, t) + \mathcal{W}_x^d(X, t)) \right). \end{aligned} \quad (23)$$

The nucleon impact factor (9) is the integral of the imaginary part of r.h.s. of eq. (23) over energy

$$\begin{aligned} I_N(k_\perp, r_\perp) = \int_0^1 \frac{d\alpha_k}{2\pi} \text{Im} \Phi_N(-(\alpha_k - \frac{r_\perp^2}{s})p_1 - k_\perp - r_\perp, \alpha_k p_1 + k_\perp) = \\ \frac{1}{3} \int_0^1 d\alpha_k \int_x^1 dX \left[s(X-x)\delta(k_\perp^2 - \alpha_k s(X-x)) - sX\delta(k_\perp^2 + \alpha_k sX) \right] \\ \left(\delta_{\lambda\lambda'} (\mathcal{V}_x^u(X, t) + \mathcal{V}_x^d(X, t)) + \frac{1}{2ms} \bar{u}(p', \lambda') \not{p}_1 \not{\epsilon}_\perp u(p, \lambda) (\mathcal{W}_x^u(X, t) + \mathcal{W}_x^d(X, t)) \right) \\ = \frac{1}{3} \int_x^1 dX \left(\delta_{\lambda\lambda'} (\mathcal{V}_x^u(X, t) + \mathcal{V}_x^d(X, t)) + \frac{1}{2ms} \bar{u}(p', \lambda') \not{p}_1 \not{\epsilon}_\perp u(p, \lambda) (\mathcal{W}_x^u(X, t) + \mathcal{W}_x^d(X, t)) \right). \end{aligned} \quad (24)$$

Since valence quark distributions decrease at $x \rightarrow 0$ we can extend the lower limit of integration in r.h.s. of eq. (24) to 0 and obtain

$$I_N(k_\perp, r_\perp) \stackrel{k_\perp^2 \gg m^2}{=} \frac{1}{3} \int_0^1 dX \left(\delta_{\lambda\lambda'} (\mathcal{V}_x^u(X, t) + \mathcal{V}_x^d(X, t)) + \frac{1}{2m_s} \bar{u}(p', \lambda') \not{p}_1 \not{\gamma}_\perp u(p, \lambda) (\mathcal{W}_x^u(X, t) + \mathcal{W}_x^d(X, t)) \right). \quad (25)$$

Let us recall the sum rules [2], [9]

$$\begin{aligned} \int_0^1 dX (\mathcal{F}_x^q(X, t) - \mathcal{F}_x^{\bar{q}}(X, t)) &= F_1^q(t) \\ \int_0^1 dX (\mathcal{K}_x^q(X, t) - \mathcal{K}_x^{\bar{q}}(X, t)) &= F_2^q(t) \end{aligned} \quad (26)$$

where $\mathcal{F}_x^q(X, t)$ and $\mathcal{K}_x^q(X, t)$ are the total (valence + sea) nonflip and spin-flip skewed quark distributions while $\mathcal{F}_x^{\bar{q}}(X, t)$ and $\mathcal{K}_x^{\bar{q}}(X, t)$ are the antiquark ones. Here $F_1^q(t)$ and $F_2^q(t)$ stand for the q -quark components of the Dirac and Pauli form factors of the proton). Since the contribution of sea quarks drops from the difference $\mathcal{F}^q - \mathcal{F}^{\bar{q}}$ we can rewrite eqs. (26) as the sum rules for valence quark distributions

$$\int_0^1 dX \mathcal{V}_x^q(X, t) = F_1^q(t), \quad \int_0^1 dX \mathcal{W}_x^q(X, t) = F_2^q(t). \quad (27)$$

Substituting this estimate to eq. (25) and using the isospin invariance, we get the final result for the nucleon impact factor at large transverse momenta

$$I_N(k_\perp, r_\perp) \stackrel{k_\perp^2 \gg m^2}{=} \delta_{\lambda\lambda'} F_1^{p+n}(t) + \frac{1}{2m_s} \bar{u}(p', \lambda') \not{p}_1 \not{\gamma}_\perp u(p, \lambda) F_2^{p+n}(t), \quad (28)$$

where $F_1^{p+n}(t) \equiv F_1^p(t) + F_1^n(t)$ and $F_2^{p+n}(t) \equiv F_2^p(t) + F_2^n(t)$. As usual, $F_1^{p(n)}$ and $F_2^{p(n)}$ are the Dirac and Pauli form factors of the proton (neutron), respectively. With our accuracy they can be approximated by the dipole formulas

$$\begin{aligned} F_1^p + \frac{t}{4m^2} F_2^p &= G_E^p = \frac{1}{\left(1 + \frac{|t|}{0.7 \text{GeV}^2}\right)^2} & F_1^p + F_2^p &= G_M^p = \frac{2.79}{\left(1 + \frac{|t|}{0.71 \text{GeV}^2}\right)^2}, \\ F_1^n + \frac{t}{4m^2} F_2^n &= G_E^n = 0 & F_1^n + F_2^n &= G_M^n = \frac{-1.91}{\left(1 + \frac{|t|}{0.71 \text{GeV}^2}\right)^2}, \end{aligned} \quad (29)$$

which leads to *

*Literally, one obtains

$$F_1^{p+n}(t) = \frac{1}{1 + \left(\frac{|t|}{0.7\text{GeV}^2}\right)^2}, \quad F_2^{p+n} = 0 \quad (31)$$

. Note that the spin-flip term turned out to be negligible for our values of t . Moreover, it vanishes at $t = 0$ which suggests that it is numerically small at all t .

Our final estimate of the nucleon impact factor is

$$I_N(k_\perp, r_\perp) \stackrel{k_\perp^2 \gg m^2}{=} \delta_{\lambda\lambda'} F_1^{p+n}(t) \quad (32)$$

where F_1^{p+n} is given by the dipole formula (31) [†]. In what follows we shall omit the factor $\delta_{\lambda\lambda'}$ (as it was done in eq. (15)) since all our amplitudes will always be diagonal in the proton's spin.

$$F_1^{p+n}(t) = \frac{1}{1 + \left(\frac{|t|}{0.71\text{GeV}^2}\right)^2} \frac{1 + 0.88 \frac{|t|}{4m^2}}{1 + \frac{|t|}{4m^2}}, \quad F_2^{p+n} = \frac{0.12}{1 + \left(\frac{|t|}{0.71\text{GeV}^2}\right)^2} \quad (30)$$

but with our accuracy we can use the estimate (31).

[†] The dipole formula for the neutron form factor does not seem to work as well as the dipole formula for the proton form factor. As a measure of the uncertainty we can compare the results obtained from eq. (31) to those obtained using the model from Ref. [15] (which was fit only to the proton form factor)

$$\begin{aligned} F_1^{p+n}(t) &= \frac{1}{3} \int_0^1 dX \left(\mathcal{V}_x^u(X, t) + \mathcal{V}_x^d(X, t) \right) \\ \mathcal{V}_x^u(X, t) &= 1.89 X^{-0.4} \bar{X}^{3.5} (1 + 6X) \exp \left(-\frac{\bar{X}}{X} \frac{|t|}{2.8\text{GeV}^2} \right) \\ \mathcal{V}_x^d(X, t) &= 0.54 X^{-0.6} \bar{X}^{4.2} (1 + 8X) \exp \left(-\frac{\bar{X}}{X} \frac{|t|}{2.8\text{GeV}^2} \right) \end{aligned} \quad (33)$$

The results for the DVCS cross section in this model are about 1.5 times bigger than the results obtained from the dipole formula (31).

IV. THE BFKL LADDER

In the next order in perturbation theory the most important diagrams are those of the type shown in Fig. (5)[‡]. Calculation of this diagrams in the leading log approximation

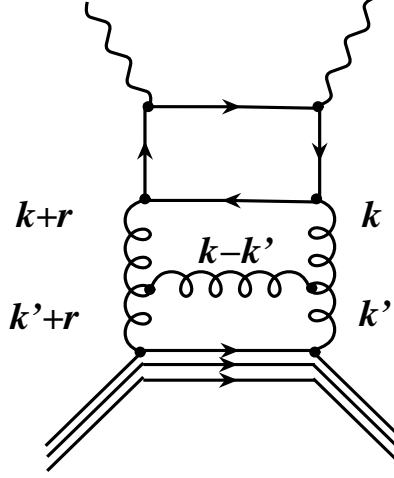


FIG. 5. Typical diagram in the next-to-leading order in perturbation theory

yields

$$V^{AB} = \frac{2sg^4}{\pi} (\sum e_q^2) \left(6\alpha_s \ln \frac{1}{x} \right) \int \frac{d^2 k_\perp}{4\pi^2} \frac{d^2 k'_\perp}{4\pi^2} \frac{I^{AB}(k_\perp, r_\perp)}{k_\perp^2 (r+k)_\perp^2} K(k_\perp, k'_\perp, r_\perp) \frac{I_N(k'_\perp, r'_\perp)}{(k'_\perp)^2 (r+k')_\perp^2} \quad (34)$$

where $K(k_\perp, k'_\perp, r_\perp)$ is the BFKL kernel [5]

$$K(k_\perp, k'_\perp, r_\perp) = -r_\perp^2 + \frac{k_\perp^2 (r-k')_\perp^2}{(k-k')_\perp^2} + \frac{k_\perp^2 (r-k')_\perp^2}{(k-k')_\perp^2} + k_\perp^2 (k-p)_\perp^2 \frac{1}{2} \delta(k_\perp - k'_\perp) \int dp_\perp \left(\frac{k_\perp^2}{p_\perp^2 (k-p)_\perp^2} + \frac{(k-r)_\perp^2}{(p-r)_\perp^2 (k-p)_\perp^2} \right) \quad (35)$$

As we shall see below, the integral over k'_\perp converges at $|k'_\perp| \gg m$ so we can again use the approximation (15) for the nucleon impact factor. One obtains

[‡]Actually, this diagram gives the total contribution in LLA if one replaces the three-gluon vertex in Fig. (5) by the effective Lipatov's vertex [11]

$$\int d^2 k'_\perp K(k_\perp, k'_\perp, r_\perp) \frac{1}{(k'_\perp)^2 (r + k')_\perp^2} I_N(k'_\perp, r'_\perp) = \pi F_1^{p+n}(t) \left(\ln \frac{k_\perp^2}{r_\perp^2} + \ln \frac{(k - r)_\perp^2}{r_\perp^2} \right) \quad (36)$$

and therefore the amplitude (34) takes the form

$$V^{AB} = \frac{g^4 s}{\pi} F_1^{p+n}(t) \left(\frac{3\alpha_s}{\pi} \ln \frac{1}{x} \right) \int \frac{d^2 k_\perp}{4\pi^2} \frac{I(k_\perp, r_\perp)}{k_\perp^2 (r + k)_\perp^2} \left(\ln \frac{k_\perp^2}{r_\perp^2} + \ln \frac{(k - r)_\perp^2}{r_\perp^2} \right). \quad (37)$$

Finally, the integration over k yields

$$\begin{aligned} V^{AB} = & \frac{2}{x} \left(\frac{\alpha_s}{\pi} \right)^2 \left(\sum_{\text{flavors}} e_q^2 \right) F_1^{p+n}(t) \left(\frac{3\alpha_s}{\pi} \ln \frac{1}{x} \right) \\ & \left((e^A, e^B)_\perp \left(\frac{1}{6} \ln^3 \frac{Q^2}{|t|} + 2 \ln \frac{Q^2}{|t|} - 2 + \zeta(3) \right) + \left(\frac{2}{r_\perp^2} (e^A, r)_\perp (e^B, r)_\perp - (e^A, e^B)_\perp \right) \right) \end{aligned} \quad (38)$$

where the accuracy is $O(\frac{1}{\ln x})$.

In the next order in BFKL approximation (see Fig. 6) it is still possible to obtain the DVCS amplitude (3) in the explicit form (we have not obtained the explicit expressions for higher-order terms in the BFKL expansion (38) [§]). The amplitude in this order is

$$\begin{aligned} V^{AB} = & \frac{g^4 s}{\pi} (\sum e_q^2) \left(6\alpha_s \ln \frac{1}{x} \right)^2 \int \frac{d^2 k_\perp}{4\pi^2} \frac{d^2 k'_\perp}{4\pi^2} \frac{d^2 k''_\perp}{4\pi^2} I(k_\perp, r_\perp) \\ & \frac{1}{k_\perp^2 (r + k)_\perp^2} K(k_\perp, k''_\perp, r_\perp) \frac{1}{(k''_\perp)^2 (r + k'')_\perp^2} K(k''_\perp, k'_\perp, r_\perp) \frac{1}{(k'_\perp)^2 (r + k')_\perp^2} I_N(k'_\perp, r'_\perp). \end{aligned} \quad (39)$$

Once again, if we use the fact that the integral over k'_\perp converges at $|k'_\perp| \gg m$ we can approximate the nucleon impact factor by eq. (32), and obtain

$$\begin{aligned} & \int \frac{d^2 k'_\perp}{4\pi^2} \int \frac{d^2 k''_\perp}{4\pi^2} K(k_\perp, k''_\perp, r_\perp) \frac{1}{(k''_\perp)^2 (r + k'')_\perp^2} K(k''_\perp, k'_\perp, r_\perp) \frac{1}{(k'_\perp)^2 (r + k')_\perp^2} I_N(k'_\perp, r'_\perp) = \\ & \frac{1}{4\pi} F_1^{p+n}(t) \int \frac{d^2 k''_\perp}{4\pi^2} \frac{K(k_\perp, k''_\perp, r_\perp)}{(k''_\perp)^2 (r + k'')_\perp^2} \left(\ln \frac{(k''_\perp)^2}{r_\perp^2} + \ln \frac{(k'' - r)_\perp^2}{r_\perp^2} \right) = \\ & \frac{1}{16\pi^2} F_1^{p+n}(t) \left(\ln^2 \frac{k_\perp^2}{r_\perp^2} + \ln^2 \frac{(k - r)_\perp^2}{r_\perp^2} \right). \end{aligned} \quad (40)$$

[§]It is possible to write down the result of the summation of the BFKL ladder in the form of Mellin integral over complex momenta using the Lipatov's conformal eigenfunctions of the BFKL equation in the coordinate space. Unfortunately, we were not able to perform explicitly the integration of the Lipatov's eigenfunctions with impact factors and without it the Mellin representation of the DVCS amplitude is useless for practical applications.

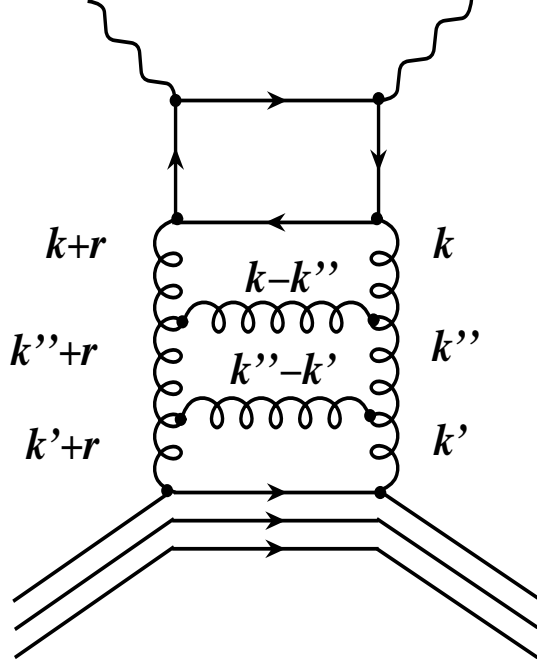


FIG. 6. Typical diagram in the next-to-next-to-leading order in perturbation theory

The resulting integration over k_{\perp} yields

$$\begin{aligned}
 V^{AB} = & \frac{9}{x} \left(\frac{\alpha_s}{\pi} \right)^4 (\sum e_q^2) F_1^{p+n}(t) \ln^2 x \left[(e^A, e^B)_{\perp} \left(\frac{1}{24} \ln^4 \frac{Q^2}{|t|} + \ln^2 \frac{Q^2}{|t|} - 2 \ln \frac{Q^2}{|t|} + \right. \right. \\
 & \left. \left. 2(\zeta(3) - 1) + 1.46 \right) + \left(\frac{2}{r_{\perp}^2} (e^A, r)_{\perp} (e^B, r)_{\perp} - (e^A, e^B)_{\perp} \right) \right]. \quad (41)
 \end{aligned}$$

As we mentioned, we were not able to obtain the explicit expressions for the amplitude in higher orders in perturbation theory. It turns out, however, that for HERA energies the achieved accuracy is reasonably good; the estimation of the next term gives $\sim 30\%$ of the answer at not too low x (see the discussion in next section). Our final result for the DVCS

amplitude with transversely polarized photons is **

$$V^{AB} = \frac{2}{x} \left(\frac{\alpha_s(Q)}{\pi} \right)^2 \left(\sum_{\text{flavors}} e_q^2 \right) F_1^{p+n}(t) \left[(e^A, e^B)_\perp v + \left(\frac{2}{r_\perp^2} (e^A, r)_\perp (e^B, r)_\perp - (e^A, e^B)_\perp \right) v' \right], \quad (42)$$

where

$$v(x, Q^2/t) = \left(\frac{1}{2} \ln^2 \frac{Q^2}{|t|} + 2 \right) + \frac{3\alpha_s(Q)}{\pi} \ln \frac{1}{x} \left(\frac{1}{6} \ln^3 \frac{Q^2}{|t|} + 2 \ln \frac{Q^2}{|t|} - 2 + \zeta(3) \right) + \frac{1}{2} \left(\frac{3\alpha_s(Q)}{\pi} \ln \frac{1}{x} \right)^2 \left(\frac{1}{24} \ln^4 \frac{Q^2}{|t|} + \ln^2 \frac{Q^2}{|t|} + 2(\zeta(3) - 1) \ln \frac{Q^2}{|t|} + 1.46 \right) \quad (43)$$

$$v'(x, Q^2/t) = 1 + \frac{3\alpha_s(Q)}{\pi} \ln \frac{1}{x} + \frac{1}{2} \left(\frac{3\alpha_s(Q)}{\pi} \ln \frac{1}{x} \right)^2. \quad (44)$$

Note that the spin-dependent part $\sim v'$ does not contain any $\ln \frac{Q^2}{|t|}$ and is hence much smaller than the spin-independent part $\sim v$. For the longitudinal polarization (13) the amplitude is twist-suppressed as $\simeq \sqrt{\frac{|t|}{Q^2}}$ so we have not calculated any terms beyond eq. (18). In the numerical analysis carried out in next sections we keep only the spin-independent part of the amplitude

$$V_\perp \equiv \frac{1}{4} \sum e_\perp^A e_\perp^B V^{AB} = \frac{2}{x} \left(\frac{\alpha_s(Q)}{\pi} \right)^2 \left(\sum_{\text{flavors}} e_q^2 \right) F_1^{p+n}(t) v(x, Q^2, t). \quad (45)$$

The above expressions give us the imaginary part of the DVCS amplitude. For the calculation of the DVCS cross section we need to know also the real part of this amplitude which can be estimated via the dispersion relation. For the positive-signature amplitude H_\perp ($\equiv \frac{1}{4} \sum e_\perp^A e_\perp^B H^{AB}$) we get [18] (see also [7])

$$\text{Re} H_\perp(s) = \frac{\pi}{2} \tan \left(s \frac{d}{ds} \right) \text{Im} H_\perp(s), \quad (46)$$

which amounts to the substitution

**In the leading logarithmic approximation it is not possible to distinguish between $\alpha_s(Q)$ and $\alpha_s(\sqrt{|t|})$ – to this end one needs to use the NLO BFKL approximation [16] (see also [17]) which is beyond the scope of this paper.

$$\ln s \rightarrow \frac{1}{2}(\ln(-s - i\epsilon) + \ln s) \quad (47)$$

in our amplitude (45). Thus, the real part is

$$\begin{aligned} R &\equiv \frac{1}{\pi} \text{Re} H_{\perp} = \frac{2}{x} \left(\frac{\alpha_s}{\pi} \right)^2 \left(\sum_{\text{flavors}} e_q^2 \right) (F_1^p(t) + F_1^n(t)) r(x, Q^2, t) \\ r(x, Q^2, t) &= \frac{\pi}{2} \left[\frac{3\alpha_s}{\pi} \left(\frac{1}{6} \ln^3 \frac{Q^2}{|t|} + 2 \ln \frac{Q^2}{|t|} - 2 + \zeta(3) \right) + \right. \\ &\quad \left. \left(\frac{3\alpha_s}{\pi} \right)^2 \ln \frac{1}{x} \left(\frac{1}{24} \ln^4 \frac{Q^2}{|t|} + \ln^2 \frac{Q^2}{|t|} + 2(\zeta(3) - 1) \ln \frac{Q^2}{|t|} + 1.46 \right) \right]. \end{aligned} \quad (48)$$

V. COMPARISON WITH THE DEEP INELASTIC SCATTERING

It is instructive to compare the DVCS amplitude V^{AB} given by eq. (3) with the corresponding amplitude for the forward γ^* scattering

$$T^{AB} = ie_{\nu}^A e_{\mu}^B \int dz e^{iqz} \langle p | T \{ j^{\mu}(z) j^{\nu}(0) \} | p \rangle. \quad (49)$$

The imaginary part of this amplitude is the total cross section for deep inelastic scattering (DIS)

$$\begin{aligned} \frac{1}{\pi} \text{Im} T^{AB} &= W^{AB} = \\ e_{\nu}^A e_{\mu}^B &\left[\left(\frac{q_{\mu} q_{\nu}}{q^2} - g_{\mu\nu} \right) F_1(x, Q^2) + \frac{1}{pq} \left(p_{\mu} - q_{\mu} \frac{pq}{q^2} \right) \left(p_{\nu} - q_{\nu} \frac{pq}{q^2} \right) F_2(x, Q^2) \right] \end{aligned} \quad (50)$$

For example W^{AB} averaged over the transverse polarizations of the photons is

$$W_{\perp} \stackrel{\text{def}}{=} \frac{1}{4} \sum e_{\perp}^A e_{\perp}^B W^{AB} = F_1(x, Q^2) = \frac{1}{2x} F_2(x, Q^2) \quad (51)$$

(at the leading twist level we have the Callan-Gross relation $F_2 = 2xF_1$). We will compare the imaginary part of the DVCS amplitude V_{\perp} given by eq. (45) to the result for W_{\perp} calculated with the same accuracy. (We use the notation $W_{\perp}(x)$ rather than $F_1(x)$ in order to avoid confusion with $F_1(t)$).

Similarly to the DVCS case, the DIS amplitude has the form (cf. eqs.(16),(34), and (39)):

$$\begin{aligned}
W_{\perp} = & \frac{2g^2 s}{\pi} \left(\sum e_q^2 \right) \int \frac{d^2 k_{\perp}}{4\pi^2} \frac{1}{k_{\perp}^4} I_{\perp}(k_{\perp}, 0) \\
& \left[1 + \frac{3g^2}{8\pi^3} \ln \frac{1}{x} \int d^2 k'_{\perp} K(k_{\perp}, k'_{\perp}, 0) + \right. \\
& \left. \frac{9g^4}{128\pi^6} \ln^2 \frac{1}{x} \int d^2 k'_{\perp} \int d^2 k''_{\perp} K(k_{\perp}, k''_{\perp}, 0) \frac{1}{(k''_{\perp})^2} K(k''_{\perp}, k'_{\perp}, 0) \right] \frac{1}{(k'_{\perp})^2} I_N(k'_{\perp}, 0) \quad (52)
\end{aligned}$$

where $I_{\perp}(k_{\perp}, 0)$ is the virtual photon impact factor averaged over the transverse polarizations [19]

$$I_{\perp}(k_{\perp}, 0) = \frac{1}{2} \int_0^1 \frac{d\alpha}{2\pi} \int_0^1 \frac{d\alpha'}{2\pi} \frac{k_{\perp}^2 (1 - 2\alpha\bar{\alpha})(1 - 2\alpha'\bar{\alpha}')}{k_{\perp}^2 \alpha' \bar{\alpha}' + Q^2 \alpha' \alpha \bar{\alpha}} \quad (53)$$

The nucleon impact factor $I_N(k'_{\perp}, 0)$ cannot be calculated in perturbation theory since it is determined by the large-scale nucleon dynamics. However, we know the asymptotics at large $k_{\perp} \gg m$

$$I_N(k_{\perp}, 0) \stackrel{k_{\perp}^2 \gg m^2}{=} F_1^{p+n}(0) = 1 \quad (54)$$

Also, at $I_N(k_{\perp}, 0) \rightarrow 0$ at $k \rightarrow 0$ due to the gauge invariance. It seems reasonable to model this impact factor by the simple formula

$$I_N(k_{\perp}, 0) = \frac{k_{\perp}^2}{k_{\perp}^2 + m^2} \quad (55)$$

which has the correct behavior both at large and small k_{\perp} . With this model, the DIS amplitude (52) takes the form

$$\begin{aligned}
W_{\perp} = & \frac{F_2}{2x} = \\
& \frac{4}{3x} \left(\frac{\alpha_s(Q)}{\pi} \right)^2 \left(\sum_{\text{flavors}} e_q^2 \right) \left[\left(\frac{1}{2} \ln^2 \frac{Q^2}{m^2} + \frac{7}{6} \ln \frac{Q^2}{m^2} + \frac{77}{18} \right) + \right. \\
& \frac{3\alpha_s}{\pi} \ln \frac{1}{x} \left(\frac{1}{6} \ln^3 \frac{Q^2}{m^2} + \frac{7}{12} \ln^2 \frac{Q^2}{m^2} + \frac{77}{18} \ln \frac{Q^2}{m^2} + \frac{131}{27} + 2\zeta(3) \right) + \frac{1}{2} \left(\frac{3\alpha_s}{\pi} \ln \frac{1}{x} \right)^2 \\
& \left. \left(\frac{1}{24} \ln^4 \frac{Q^2}{m^2} + \frac{7}{36} \ln^3 \frac{Q^2}{m^2} + \frac{77}{36} \ln^2 \frac{Q^2}{m^2} + \left(\frac{131}{27} + 4\zeta(3) \right) \ln \frac{Q^2}{m^2} + \frac{1396}{81} - \frac{\pi^4}{15} + \frac{14}{3} \zeta(3) \right) \right]. \quad (56)
\end{aligned}$$

Note that the coefficients in front of leading logs of Q^2 , determined by the anomalous dimensions of twist-2 operators, coincide up to the factor 2/3. The graph of the model (56)

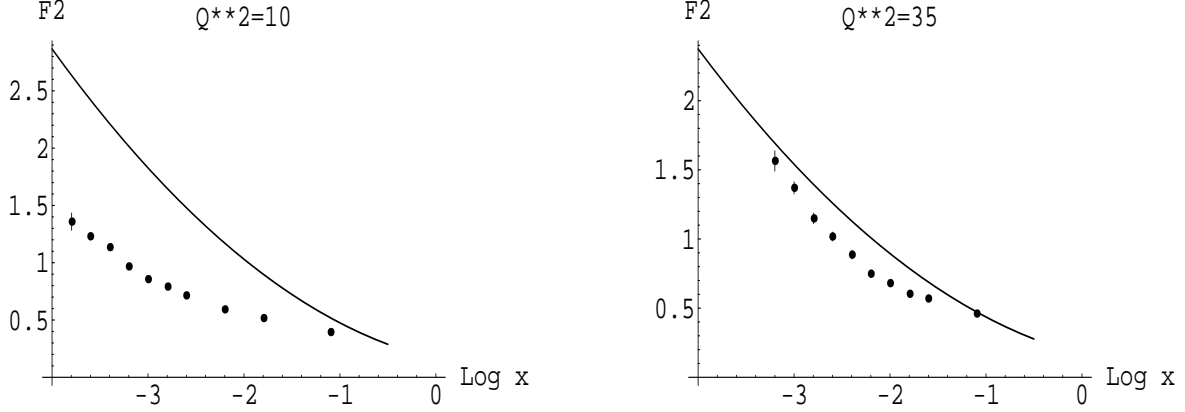


FIG. 7. $F_2(x)$ from eq. (56) versus experimental data at $Q^2 = 10\text{GeV}^2$ and $Q^2 = 35\text{GeV}^2$

versus the experimental data is presented in Fig. 7 for $Q^2 = 10\text{GeV}^2$ and $Q^2 = 35\text{GeV}^2$ (we take $\sum e_q^2 = \frac{10}{9}$).

In the case of DIS it is possible to calculate explicitly the next term in BFKL series (56)^{††}. It has the form

$$\frac{4}{3x} \left(\frac{\alpha_s(Q)}{\pi} \right)^2 \left(\sum_{\text{flavors}} e_q^2 \right) \left[\frac{1}{6} \left(\frac{3\alpha_s}{\pi} \ln \frac{1}{x} \right)^3 \left(\frac{1}{120} \ln^5 \frac{Q^2}{m^2} + \frac{7}{144} \ln^4 \frac{Q^2}{m^2} + \frac{77}{108} \ln^3 \frac{Q^2}{m^2} + \left(\frac{131}{54} + 3\zeta(3) \right) \ln^2 \frac{Q^2}{m^2} + \left(\frac{1396}{81} - \frac{\pi^4}{15} + 7\zeta(3) \right) \ln \frac{Q^2}{m^2} + \frac{4736}{243} - \frac{7\pi^4}{90} + \frac{77}{3} \zeta(3) + 6\zeta(5) \right) \right] \quad (57)$$

The ratio of this $(\alpha_s \ln x)^3$ term to the sum of the first three ones (56) is presented in Fig. 8 for $Q^2 = 10\text{GeV}^2$ and $Q^2 = 35\text{GeV}^2$. From these graphs we see that the sum of the first tree terms gives the reliable estimate of the DIS amplitude at not too low x and it is expected that the same will also be true for DVCS amplitude^{‡‡}.

^{††}For DIS it is possible to write down the total BFKL sum as a Mellin integral and unlike DVCS the integrals of impact factors with the BFKL eigenfunctions $(k_\perp^2)^{-\frac{1}{2}+i\nu}$ can be calculated explicitly. Eqs. (56) and (57) correspond to the expansion of this explicit expression in powers of $\alpha_s \ln x$.

^{‡‡} At very small $x \sim 10^{-3} \div 10^{-5}$ the full BFKL result for F_2 in our model is growing more rapidly than Fig. 7. On the other hand if one takes into account the NLO BFKL corrections [16] [17] the result for F_2 at very small x goes well under the experimental points. This indicates that at such

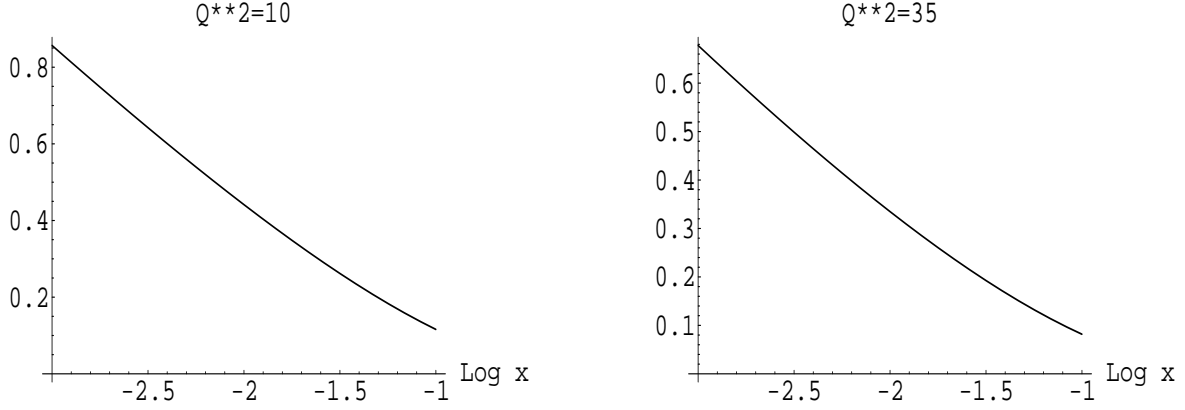


FIG. 8. The ratio of the $\ln^3 x$ term (57) to eq. (56) at $Q^2 = 10\text{GeV}^2$ and $Q^2 = 35\text{GeV}^2$

It is instructive to compare the t -dependence of our DVCS amplitude (43) with the model used in the paper [7]

$$V_1(x, t, Q^2) = \frac{1}{R} F_1(x, Q^2) e^{bt/2} \quad (58)$$

$$V_2(x, t, Q^2) = \frac{1}{R} F_1(x, Q^2) \frac{1}{(1 + \frac{|t|}{0.71})^2} \quad (59)$$

where $R \simeq 0.5$ for our energies. (Literally, the model used in ref. [7] corresponds to V_1 but it is more natural to approximate the t - dependence by the dipole formula [22]). The comparison is shown in Fig. 9 for $Q^2 = 10\text{GeV}^2$, $Q^2 = 35\text{GeV}^2$ and $x=0.01$, $x=0.001$.

VI. DVCS CROSS SECTION

In order to estimate the cross section for DVCS at HERA kinematics ($Q^2 > 6\text{GeV}^2$ and $x < 10^{-2}$) we will use formulas from Ref. [7] (see also Ref. [23]) with the trivial substitution $\frac{1}{2x} F_2(x) R^{-1} e^{bt/2} \rightarrow V_\perp(x, Q^2, t)$. The expressions for the DVCS cross section, the QED

x we need to unitarize the BFKL pomeron, which is currently an unsolved problem. (The best hope is to find the effective action for the BFKL pomeron (see e.g. [20], [21])). On the contrary, at “intermediate” $x \sim 0.1 \div 0.001$, we see from Fig. 7 that, since the corrections almost cancel each other, it makes sense to take into account only a few first terms in BFKL series.

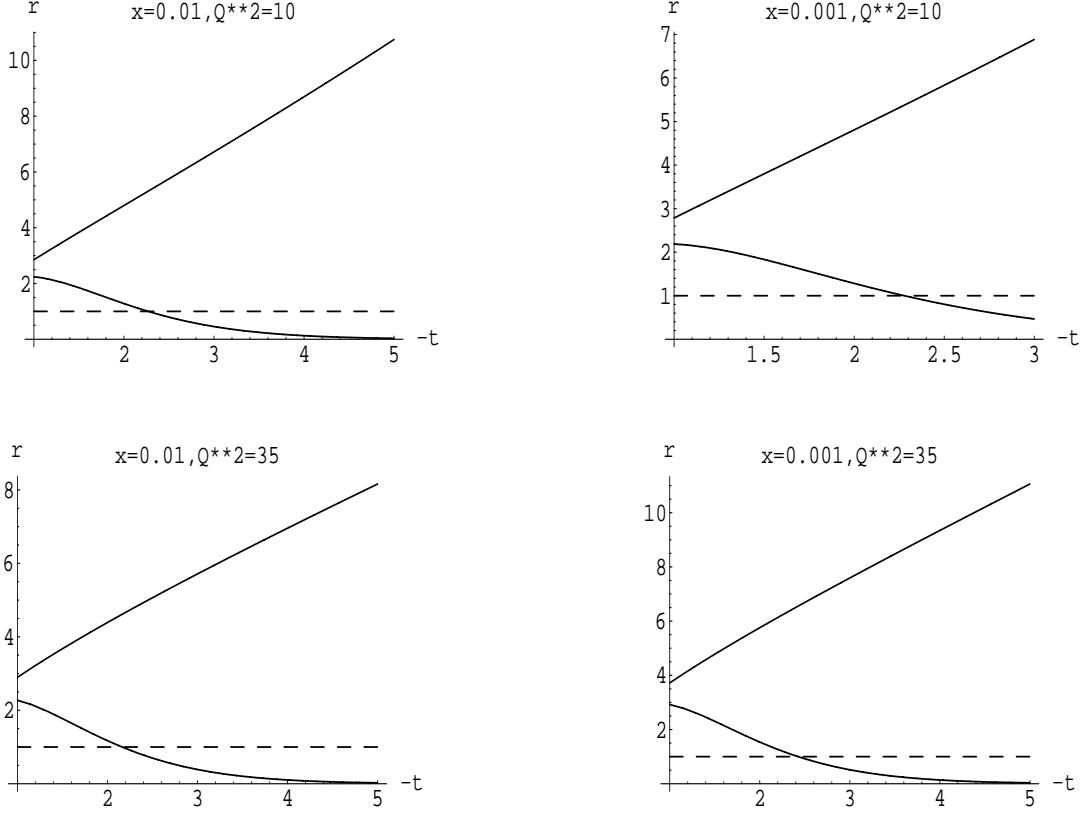


FIG. 9. The ratio V_1/V_\perp (lower curve) and V_2/V_\perp (upper curve).

Compton (Bethe-Heitler) cross section, and the interference term have the form ($\bar{y} \equiv 1 - y$)
§§:

$$\frac{d\sigma^{\text{DVCS}}}{dx dy dt d\phi_r} = \pi \alpha^3 x \frac{1 + \bar{y}^2}{Q^4 y} (V_\perp^2(x, Q^2, t) + R_\perp^2(x, Q^2, t)) \quad (60)$$

$$\frac{d\sigma^{\text{QEDC}}}{dx dy dt d\phi_r} = \frac{\alpha^3}{\pi x} \frac{y(1 + \bar{y}^2)}{|t| Q^2 \bar{y}} \left((F_1^p(t))^2 + \frac{|t|}{4m^2} (F_p^2(t))^2 \right) \quad (61)$$

$$\frac{d\sigma^{\text{INT}}}{dx dy dt d\phi_r} = \mp 2\alpha^3 \frac{(1 + \bar{y}^2)}{Q^3 \sqrt{\bar{y}|t|}} R_\perp(x, Q^2, t) F_1^p(t) \cos \phi_r. \quad (62)$$

Here $y = 1 - \frac{E'}{E}$ (E and E' are the incident and scattered electron energies, respectively, as defined in the proton rest frame) and $\phi_r = \phi_e + \phi_N$ where ϕ_N is the azimuthal angle between the plane defined by γ^* and the final state proton and the $x - z$ plane and ϕ_e is the azimuthal angle between the plane defined by the initial and final state electron and

§§The expression for the interference term from ref. [7] is corrected by factor 2 [22], [25]

$x - z$ plane (see Ref. [7]). As mentioned above, we approximate the Dirac and Pauli form factors of the proton by the dipole formulas (29).

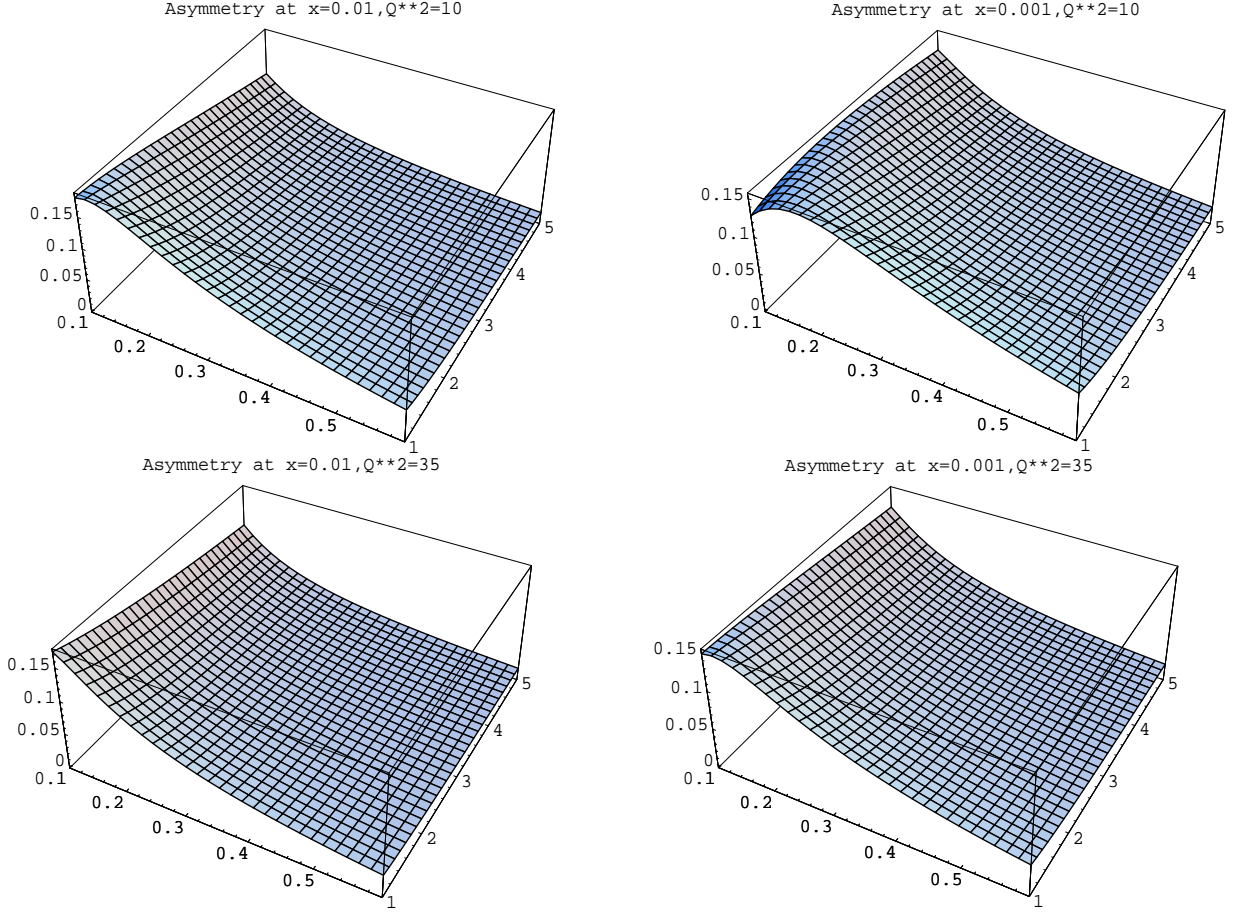


FIG. 10. Asymmetry versus $y = 0.1 \div 0.6$ and $|t| = 1 \div 5 \text{ GeV}^2$.

At first let us discuss the relative weight of the above cross sections. We start with the asymmetry defined in ref. [24]

$$A = \frac{\int_{-\pi/2}^{\pi/2} d\phi_r d\sigma^{\text{DQI}} - \int_{\pi/2}^{3\pi/2} d\phi_r d\sigma^{\text{DQI}}}{\int_0^{2\pi} d\phi_r d\sigma^{\text{DQI}}} \quad (63)$$

where

$$d\sigma^{\text{DQI}} \equiv d\sigma^{\text{DVCS}} + d\sigma^{\text{QEDC}} + d\sigma^{\text{INT}}. \quad (64)$$

The asymmetry shows the relative importance of the interference term, which is proportional to the real part of the DVCS amplitude. In our approximation the asymmetry is

$$A(y, t) = \frac{4y \sqrt{\frac{Q^2}{|t|\bar{y}}} (\sum e_q^2) \left(\frac{\alpha_s}{\pi}\right)^2 \left(1 + 2.8 \frac{|t|}{4m^2}\right) r}{4\pi^2 (\sum e_q^2)^2 (v^2 + r^2) \left(\frac{\alpha_s}{\pi}\right)^4 \left(1 + \frac{|t|}{4m^2}\right) + \frac{y^2 Q^2}{\bar{y}|t|} \left(1 + 7.84 \frac{|t|}{4m^2}\right)} \quad (65)$$

The plots of asymmetry versus y and $|t|$ are given by Fig. 10.

Second, we define the ratio of the DVCS and Bethe-Heitler cross sections [7]

$$D(y, t) \equiv \frac{d\sigma_{DVCS}}{d\sigma_{QEDC}} = \frac{4\pi^2 (\sum e_q^2)^2 (v^2 + r^2) \left(\frac{\alpha_s}{\pi}\right)^4 \left(1 + \frac{|t|}{4m^2}\right) \bar{y} \frac{|t|}{Q^2}}{y^2 \left(1 + 7.84 \frac{|t|}{4m^2}\right)} \quad (66)$$

This ratio is presented on Fig. 11. We see that there is a sharp dependence on y ; at $y > 0.2$

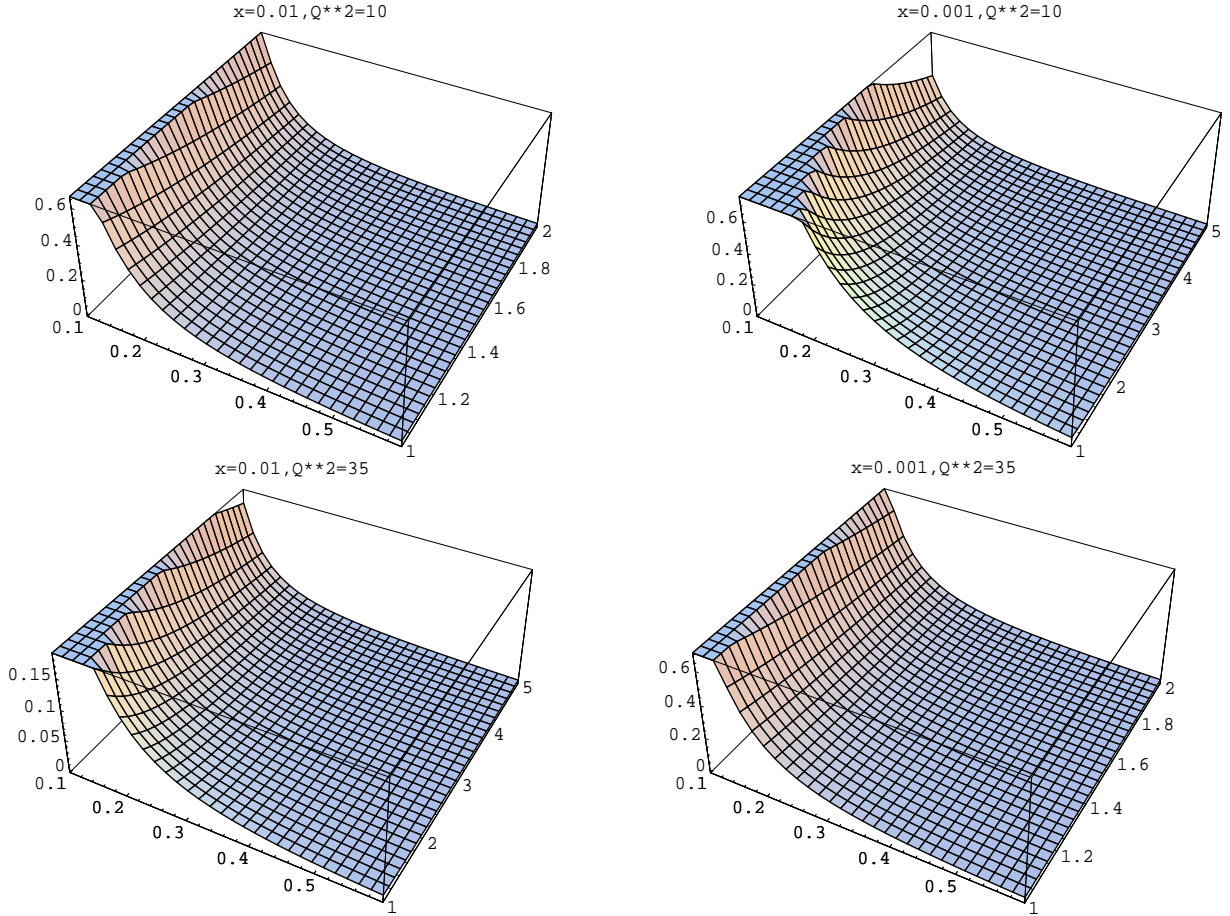


FIG. 11. The ratio $D(x, Q^2/t)$ versus $y = 0.1 \div 0.6$ and $|t| = 1 \div 5 \text{ GeV}^2$

the DVCS part is negligible in comparison to Bethe-Heitler background whereas at $y < 0.05$ the QEDC background is small in comparison to DVCS.

Finally let us estimate the relative weight of the DVCS signal (starting from $|t| = 1$ GeV²) as compared to the DIS background. We define (cf. ref. [7])

$$R_\gamma = \frac{\sigma(\gamma^* + p \rightarrow \gamma + p)}{\sigma(\gamma^* + p \rightarrow \gamma^* + p)} \simeq \frac{4\pi\alpha}{Q^2 F_2(x, Q^2)} \left(\frac{\alpha_s}{\pi}\right)^4 \left(\sum e_q^2\right)^2 \int_1^{Q^2} dt \left(F_1^{p+n}(t)\right)^2 (v^2(x, Q^2/t) + r^2(x, Q^2/t)) \quad (67)$$

At $Q^2 = 10\text{GeV}^2$ we find $R_\gamma = 1.56 \times 10^{-5}$ for $x = 0.01$ and $R_\gamma = 2.36 \times 10^{-5}$ for $x = 0.001$, while for $Q^2 = 35\text{GeV}^2$ we find $R_\gamma = 0.62 \times 10^{-5}$ for $x = 0.01$ and $R_\gamma = 0.71 \times 10^{-5}$ for $x = 0.001$.

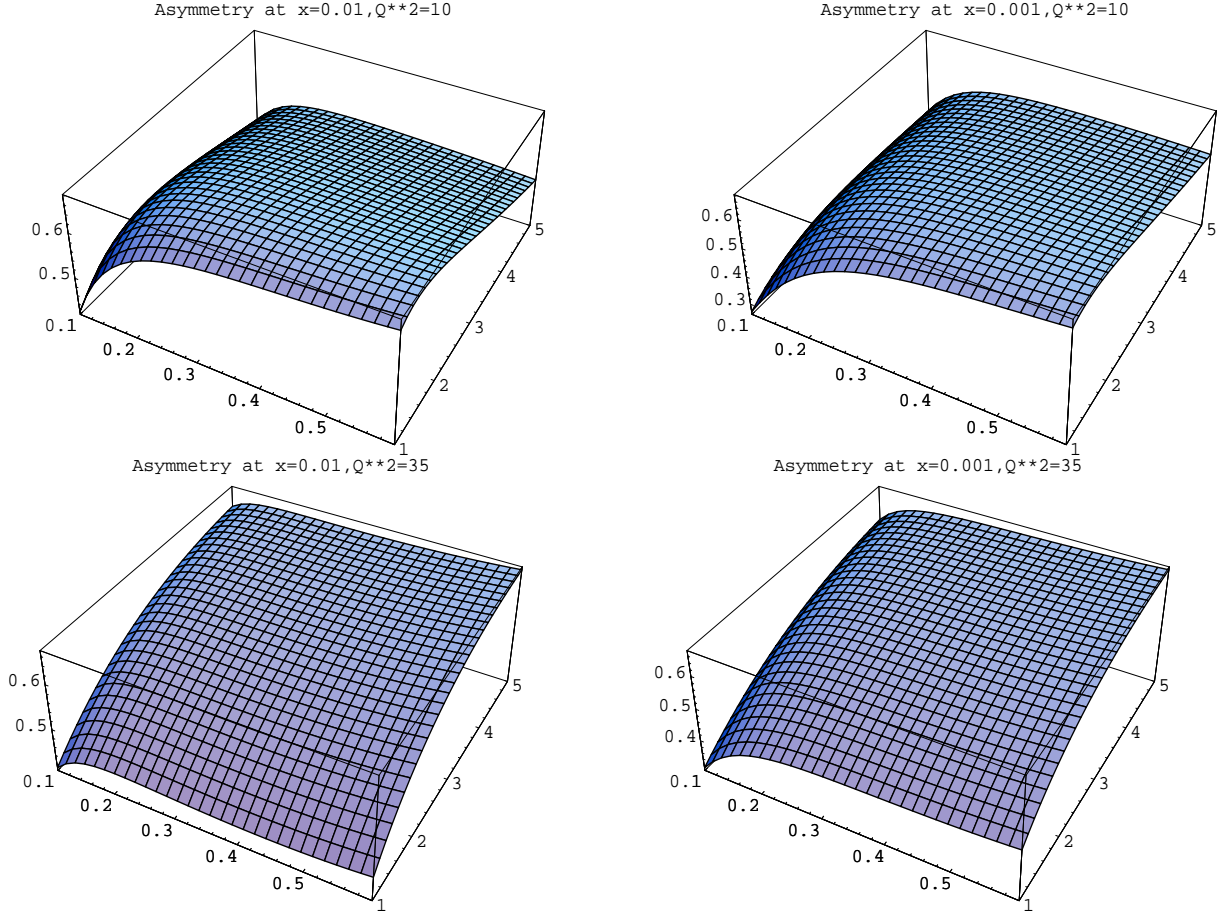


FIG. 12. Asymmetry with the correction factor (68).

The expressions (60)-(62) are correct if $Q^2 \ll |t|$ up to $O(\frac{|t|}{Q^2})$ accuracy with the notable exception of the correction $O(\frac{\sqrt{|t|}}{Q})$ coming from the expansion of electron propagator in the

u-channel of the Bethe-Heitler amplitude. As suggested in ref. [25], at intermediate t one can keep the propagator in unexpanded form (and expand the rest of the amplitude, as we have done above). This amounts to the replacement

$$\bar{y} \rightarrow \bar{y} \left[\left(1 + \frac{|t|}{Q^2 \bar{y}}\right) \left(1 + \frac{|t| \bar{y}}{Q^2}\right) - 2 \frac{(2-y)}{\sqrt{\bar{y}}} \sqrt{\frac{|t|}{Q^2}} \cos \phi_r + 4 \frac{|t|}{Q^2} \cos^2 \phi_r \right] \quad (68)$$

in the numerator in eqs. (61) and (62) (see ref. [23]). The resulting asymmetry (63) is

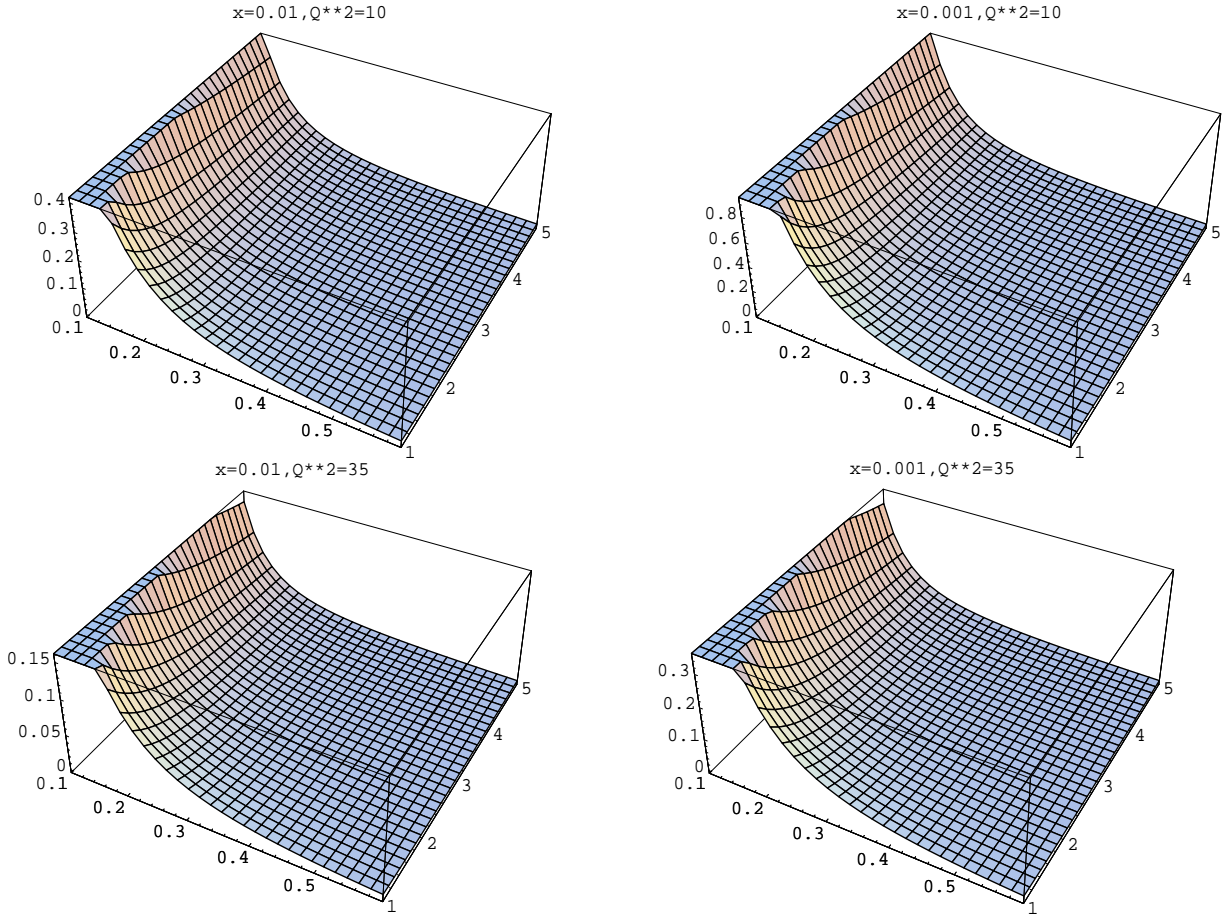


FIG. 13. The ratio $D(x, Q^2/t)$ with the correction factor (68).

presented in Fig. 12. We see that the correction factor (68) crucially changes the behavior of the asymmetry due to the fact that it restores the azimuthal dependence of the QEDC amplitude which was not taken into account in eqs. (60-62). In order to find asymmetry at these Q^2 and t with greater accuracy one should take into account other twist-4 contributions

as well. On the contrary, the ratio $D(x, Q^2/t)$ does not change much (see Fig. 13) so we hope that our leading-twist results for the ratio presented in Fig. 11 are reliable.

VII. CONCLUSION

The DVCS in the kinematical region (1) is probably the best place to test the momentum transfer dependence of the BFKL pomeron. Without this dependence, the model (59) would be exact, hence the upper curves in Fig. 9 indicate how important is the t -dynamics of the pomeron. We see that the t -dependence of the BFKL pomeron changes the cross section at $t > 2\text{GeV}^2$ by orders of magnitude and therefore it should be possible to detect it.

The pQCD calculation of the DVCS amplitude in the region (1) is in a sense even more reliable than the calculation of usual DIS amplitudes since it does not rely on the models for nucleon parton distributions. Indeed, all the non-perturbative nucleon input is contained in the Dirac form factor of the nucleon ***, which is known to a pretty good accuracy. (Of course any reasonable models of nucleon parton distributions such as (24) should reproduce the form factor after integration over X).

Finally, let us discuss uncertainties in our approximation and possible ways to improve it. One obvious improvement would be to calculate (at least numerically) the next $\sim (\alpha_s \ln x)^3$ term in the BFKL series for the DVCS amplitude. Hopefully, it will be as small as the corresponding calculation of the DIS amplitude suggests. Second, there are non-perturbative corrections to the BFKL pomeron which we mention above. These non-perturbative corrections correspond to the situation like the “aligned jet model” when one of the two gluons in Fig. (1) is soft and all the momentum transfers through the other gluon. It is not clear how to take these corrections into account, but one should expect them to be smaller than the corresponding corrections to $F_2(x)$ which come from two non-perturbative gluons in Fig. 1

*** There are, of course, the non-perturbative corrections to the BFKL pomeron itself. At present, it is not clear how to take them into account.

(in other words, from the “soft pomeron” contribution to $F_2(x)$).

The biggest uncertainty in our calculation is the argument of coupling constant α_s which we take to be Q^2 . As we mention above, it is not possible to fix the argument of α_s in the LLA, so we could have used $\alpha_s(|t|)$ instead. We hope to overcome this difficulty by using the results of NLO BFKL in our future work.

ACKNOWLEDGMENTS

The authors are grateful to A.V. Belitsky, C.E. Hyde-Wright, I.V. Musatov, A.V. Radyushkin, and M.I. Strikman for valuable discussions. This work was supported by DOE contract DE-AC05-84ER40150 under which the Southeastern Universities Research Association (SURA) operates the Thomas Jefferson National Accelerator Facility.

REFERENCES

-
- [1] D.Muller, D.Robaschik, B. Geyer, F.M. Dittes, and J. Horejsi, *Fortschr.Phys.* **42**, 101 (1994)
 - [2] X. Ji, *Phys. Lett. B* **78**, 610 (1997), *Phys. Rev. D* **55**, 7114 (1997)
 - [3] A.V. Radyushkin, *Phys. Lett. B* **380**, 417 (1996), *Phys. Lett. B* **385**, 333 (1996)
 - [4] J. Bartels and M. Loewe, *Z. Phys. C* **12**, 263 (1982)
 - [5] V.S. Fadin, E.A. Kuraev, and L.N. Lipatov, *Phys. Lett. B* **60**, 50 (1975);
I.I. Balitsky and L.N. Lipatov, *Sov. Journ. Nucl. Phys.* **28**, 822 (1978)
 - [6] [ZEUS Collaboration], *Observation of DVCS in e^+ Interactions at HERA*, paper submitted to EPS HEP99 Conference, Tampere, 1999 (see also <http://www-zeus.desy.de>)
 - [7] L.L. Frankfurt, A. Freund, and M.I. Strikman, *Phys. Rev. D* **58**, 114001 (1998), Erratum-
Phys. Rev. D **59**, 119901 (1999)

- [8] P.A.M. Guichon, M. Vanderhaeghen, *Prog.Part.Nucl.Phys.* **41**, 125 (1998)
- [9] A.V. Radyushkin, *Phys. Rev. D* **56**, 5524 (1997)
- [10] J.C. Collins, L.L. Frankfurt, and M.I. Strikman, *Phys. Rev. D* **56**, 2982 (1997)
- [11] L.N. Lipatov, *Phys. Reports* **286**, 131 (1997).
- [12] H. Cheng and T.T. Wu, *Phys. Rev.* **182**, 1852 (1969), *Phys. Rev. D* **1**, 2775 (1970); V.N. Gribov et al., *Sov. J. Nucl. Phys.* **12**, 543 (1971).
- [13] I. Balitsky, *Nucl. Phys. B* **463**, 99 (1996).
- [14] I. Balitsky, *Phys. Lett. B* **124**, 230 (1983).
- [15] A.V. Radyushkin, *Phys. Rev. D* **58**, 114008 (1998)
- [16] L.N. Lipatov and V.S. Fadin, *Phys. Lett. B* **429**, 127 (1998), *Nucl. Phys. B* **477**, 767 (1997), *Nucl. Phys. B* **406**, 259 (1993)
- [17] G. Carnici and M. Ciafaloni, *Phys. Lett. B* **412**, 396 (1997), *Phys. Lett. B* **430**, 349 (1998)
- [18] J.B. Bronzan, G.L. Kane, and U.P. Sukhatme, *Phys. Lett. B* **49**, 272 (1974).
- [19] I.I. Balitsky and L.N. Lipatov, *JETP Letters* **30**, 355 (1979).
- [20] L.N. Lipatov, *Nucl. Phys. B* **452**, 369 (1996)
- [21] I. Balitsky, *Phys. Rev. D* **014020**, 60 (1999).
- [22] M.I. Strikman, private communication.
- [23] M. Diehl, T. Gousset, B. Pire, J.P. Ralston *PLB* **411**, 193 (1997).
- [24] L.L. Frankfurt, A. Freund, and M.I. Strikman, *Phys. Lett. B* **460**, 417 (1999)
- [25] A.V. Belitsky, D. Mueller, L. Niedermeier, and A. Shaefer, hep-ph/0004059.